Journal Name

ARTICLE

A Frustrated Ferrimagnet $Cu_5(VO4)_2(OH)_4$ with 1/5 Magnetization Plateau on a New Spin-Lattice of Alternant Triangular Strip and Honeycomb Strip

Received 00th January 20xx,
Accepted 00th January 20xx

DOI: 10.1039/x0xx00000x

www.rsc.org/

Su-Yun Zhang,[a] Wen-Bin Guo,[a] Ming Yang,[a] Ying-Ying Tang,[a,b] Mei-Yan Cui,[a,b] Nan-Nan Wang,[a] Zhang-Zhen He[*,a]

$Cu_5(VO_4)_2(OH)_4$ (turanite) is a layered compound, exhibiting a copper(Ⅱ) oxide layer in the [0 1 1] plane composed of edge-sharing CuO_6 octahedra. Each Cu-O layer is further separated by VO_4 tetrahedra. Closer scrutiny found that the copper(Ⅱ) oxide layer in the compound represents a totally new geometrically-frustrated lattice, the 1/6 depleted triangular lattice. More specifically, the spin network in the [0 1 1] plane is formed by the alternant ranking of triangular strips and honeycomb strips. Magnetic measurements show that $Cu_5(VO_4)_2(OH)_4$ behaves as a spin-1/2 ferrimagnet with T_c = ~ 4.5 K. It exhibits unusual 1/5 magnetization plateau arising from the competition between antiferromagnetic and ferromagnetic interactions caused by strong frustration. The possible spins are also arranged.

Introduction

Quasi-two-dimensional (2D) materials have attracted great scientific attention as the discovery of high-temperature superconductivity in quasi-2D cuprates and their correlations with the spin-fluctuation of antiferromagnets. Usually quasi-2D magnetic materials show various fascinating and unique magnetic phenomena originating from their particular geometry of spin networks built by magnetic ions. For example, the quasi-2D La_2CuO_4, a quantum Heisenberg antiferromagnet on a square lattice, is the parent compound of high-T_c cuprates.[1] The Wigner crystallization of magnons is realized in 2D orthogonal dimer system $SrCu_2(BO_3)_2$[2] while the Bose-Einstein condensation of magnons is observed in 2D bilayer system $BaCuSi_2O_6$[3].The correlation of magnetic properties and nontrivial topology features has given an exciting issue in chemistry and physics.

Currently, most interest is focused on quasi-2D magnetic systems with triangular, kagomé and honeycomb lattices since the striking presence of geometric frustrations in these systems give rise to variety of exotic ground states.[4-10] In the representative quasi-2D magnetic systems with a triangular lattice, a low-temperature spin-disordered state stabilized by geometrical frustration is observed in $NiGa_2S_4$[11] whereas Cs_2CuCl_4 is an example of "dimensional reduction" induced by frustration and quantum fluctuations.[12] Amongst possible quasi-2D structures, the kagomé lattice has attracted special attention because magnetic systems in such lattice are the most promising candidates possessing an resonating valence bond (RVB) "spin-liquid" state, as observed in herbertsmithite, $ZnCu_3(OH)_6Cl_2$ and its analogues.[13-16] Besides, the few studies on the properties of compounds with distorted kagomé lattice have exhibited interesting properties such as spin glass behavior,[17] orbital switching,[18] orbital fluctuations and orbital-ordering transition,[19] magnetically driven ferroelectric order,[20] magnetization plateau,[21,22] short-range antiferromagnetic (AF) ordering.[23] Another special variety of the geometry is the honeycomb net. System on an ideal AF honeycomb lattice with only AF nearest-neighbor interaction is free from frustration; however, it turns out to be frustrated if the next-nearest interaction is also AF.[24] Exactly as in $Bi_3M_4O_{12}(NO_3)$ with an ideal honeycomb-lattice, no AF LRO was found down to 0.4 K because of the magnetic frustration due to the presence of nextnearest AF interaction.[25] Different behaviors appear in the case of honeycomb-layered cuprates, delafossite-derived Cu_5SbO_6, $NaFeO_2$-derived $Na_3Cu_2SbO_6$ and $Na_2Cu_2TeO_6$, in which strong S = 0 Cu^{2+}–Cu^{2+} dimers formed across a subset of the shared edges of the octahedra in the honeycomb plane.[26-28] In short, the magnetic behavior of quasi-2D systems is greatly affected by the geometry of magnetic lattice and the continuing search for compounds with new quasi-2D spin lattices is of great interest.

$Cu_5(VO_4)_2(OH)_4$ (mineral name, turanite) crystallizes in a triclinic structure of space group *P*-1 with a = 5.3834(2), b = 6.2736(3), c = 6.8454(3), and α = 86.169(1), β = 91.681(1), γ = 92.425(1).[29] The nanobelts of turanite has been synthesized

[a] State Key Laboratory of Structural Chemistry, Fujian Institute of Research on the Structure of Matter, Chinese Academy of Sciences, Fuzhou 350002, P. R. China
[b] University of the Chinese Academy of Sciences, Beijing, 100039, People's Republic of China
† E-mail: hezz@fjirsm.ac.cn. Fax: +86-591-63176255.
Electronic Supplementary Information (ESI) available: Profile coefficients used for Rietveld refinements of X-ray powder patterns, unit cell parameters and residuals after Rietveld refinements of $Cu_5(VO_4)_2(OH)_4$ (Table S1), simulated and experimental XRD patterns (Figure S1), EDS (Figure S2), IR (Figure S3), TG (Figure S4), plot of d*χ*/d*T* (Figure S5), AC magnetization (Figure S6). See DOI: 10.1039/x0xx00000x

and reported to be a promising anode candidate for the application in lithium-ion batteries with higher specific capacity, high Coulombic efficiency, and good cycle stability.[30] To the best of our knowledge, magnetic studies of $Cu_5(VO_4)_2(OH)_4$ has never been done so far. What is more, it exhibits a novel spin-lattice, the 1/6 depleted triangular lattice and no experimental realization of such lattice is known. In this paper, we report on the exotic magnetic properties of $Cu_5(VO_4)_2(OH)_4$.

Experimental Section

Reagents and instrumentation.

$Cu(CH_3COO)_2(H_2O)$ (>99.9%) and Na_3VO_4 (>99.9%) were purchased from Aladdin Chemistry Co. Ltd. and used without further purification. X-ray diffraction (XRD) patterns of powder samples were collected on a Rigaku MiniFlex II diffractometer using monochromated Cu Kα radiation (λ= 1.540598 Å) at room temperature in the angular range of 2θ = 5–85° with a step size of 0.02°. Microprobe elemental analyses were performed on a field emission scanning electron microscope (FESEM, SUB-8010) equipped with an energy dispersive X-ray spectroscope (EDS, Oxford INCA). Elemental analysis (EA) was performed on a Vario EL III elemental analyser. IR spectrum was recorded on a Magna 750 FT-IR spectrometer as KBr pellets in the range of 4000-400 cm^{-1}. Thermogravimetric analysis (TGA) was carried out with a NETZSCH STA 449C unit at a heating rate of 15 ℃/min under nitrogen atmosphere.

Magnetic and heat capacity measurements were performed using a commercial Quantum Design Physical Property Measurement System (PPMS or MPMS). Powdered samples (25.24 mg) of $Cu_5(VO_4)_2(OH)_4$ were placed in a gel capsule sample holder which was suspended in a plastic drinking straw. Magnetic susceptibility was measured at 0.1 T from 300 to 2 K. Magnetization was measured at 2 K and in applied field from -8 to 8 T (field scan of 0.1 T/step). Heat capacity was measured at zero field by a relaxation method using a pellet sample (~2.0 × 2.0 mm^2, 7.62 mg).

Synthesis of $Cu_5(VO_4)_2(OH)_4$.

Polycrystalline sample of $Cu_5(VO_4)_2(OH)_4$ were synthesized by a hydrothermal method. A mixture of $Cu(CH_3COO)_2(H_2O)$ (0.0544 g, 0.4 mmol) and Na_3VO_4 (0.0364 g, 0.2 mmol) was dissolved in 6 mL distilled water. The pH value of the mixture was adjusted to 8.2 by adding 28% aqueous ammonia solution dropwise. Then the mixture was sealed in a 28 ml PTEE-lined stainless steel vessel and heated at 200 °C for 72 h. After cooling to room-temperature, green powder of $Cu_5(VO_4)_2(OH)_4$ were obtained by filtration. Its purity was confirmed by powder X-ray diffraction technique (Figure S1). The energy-dispersive spectrometry (EDS) elemental analyses on polycrystalline sample indicated the existence of Cu and V, with an average molar ratio of Cu/V of 2.4: 1.0 (Figure S2). Elemental analysis (%): H 0.65; found: H 0.69, which is in good agreement with the one determined from the reported $Cu_5(VO_4)_2(OH)_4$. IR data give peaks at (KBr cm^{-1}): 454 (s), 765 (s),

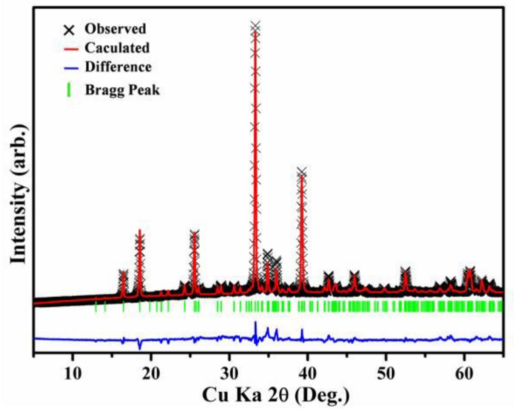

Figure 1. Rietveld refinement plot of the XRD powder patterns of $Cu_5(VO_4)_2(OH)_4$. The symbol (×) represents the observed data, and the red solid line is the calculated pattern; the difference curve is drawn as blue and the green short vertical bars are the reflection positions.

829 (w), 886 (s), 3309 (s), indicating the existence of VO_4^{3-} and OH^- (Figure S3). TGA analysis exhibits that 6.4% of the weight is lost at about 300-485°C, corresponding to the release of OH^- in the form of water molecule (5.9%) in $Cu_5(VO_4)_2(OH)_4$ (Figure S4). Besides, a whole-powder profile fitting procedure using the program GSAS by the Rieltveld refinements was performed.[31,32] Nine profile parameters were used for refinements, and unit cell parameters are refined with atomic positions fixed. Details of XRD pattern refinements are summarized in Table S1, Supporting Information. As the plot from the Rietveld refinements fits well with the measurement powder XRD diffraction patterns and the lattice parameters suggested by these procedures are very approximate to that obtained by single-crystal X-ray diffraction, the purities of synthetic sample were further confirmed (Figure 1).

Results and discussion

Spin-lattice Description. Detailed descriptions of the crystal structure of $Cu_5(VO_4)_2(OH)_4$ are reported as in ref. 29. Herein,

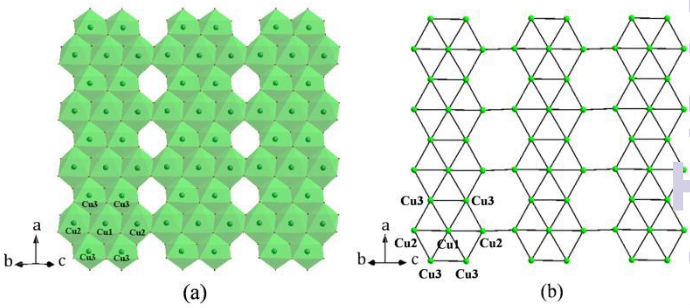

Figure 2. (a) Structural framework of $Cu_5(VO_4)_2(OH)_4$, where polyhedra, large balls, and small balls represent the CuO_6, Cu, and O, respectively. The three different Cu sites are labeled. (b) Spin lattice of Cu^{2+} ions in the [0 1 1] plane of $Cu_5(VO_4)_2(OH)_4$.

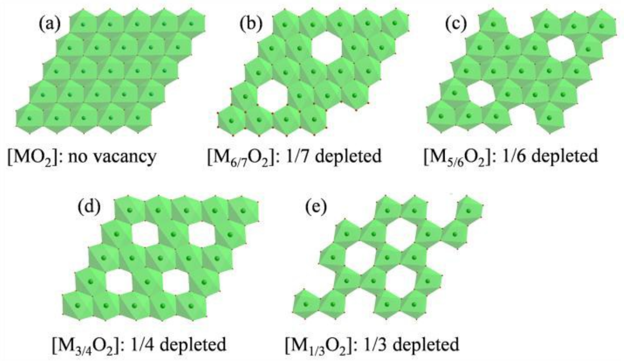

Figure 3. Comparison of (a) triangular, (b) maple-leaf, (c) spin lattice in $Cu_5(VO_4)_2(OH)_4$, (d) Kagomé, (e) honeycomb lattice.

we will describe the 2D spin-lattice formed by Cu^{2+} briefly. As shown in Figure 2a, Cu^{2+} ions of $Cu_5(VO_4)_2(OH)_4$ have three different Wyckoff sites. Cu(1) is sitting on the 2i site; Cu(2) and Cu(3) are on general sites. The interconnection of Cu(2) and Cu(3) forms a distorted honeycomb lattice made up of two types of hexagons ($Cu(2)_2Cu(3)_4$ and $Cu(2)_4Cu(3)_2$), which arranged along *a*-axis, respectively, forming two hexagon bands alternate along (0 1 1) direction. Cu(1) is located at the center of $Cu(2)_2Cu(3)_4$ hexagons, resulting in a striped triangular lattice along *a*-axis.

Most intriguingly, it is a new variant of triangular lattice and now we will discuss the well-known octahedral 2D lattices related to the parent triangular lattice by incremental depletion as shown in Figure 3.[33,34] Triangular lattice can be expressed as $[MO_2]$. 1/7 of the M sites in triangular lattice depleted orderly gives birth to the malpe leaf lattice, in which edge-shared triangles encompass "isolated" hexagon; the ordering of 1/4 of M vacancies leads to Kagomé lattice made up of corner-sharing triangles, and that of 1/3 of vacancies forms honeycomb lattice with only edge-sharing hexagons. In the lattice of $Cu_5(VO_4)_2(OH)_4$, the ordering of 1/6 of M vacancies gives birth to a new spin lattice composed of alternate triangular strips and honeycomb strips. It is obvious that the gradually increase of M vacancies resulted in the continuous decrease of triangles in the lattice which will influence the magnetic properties directly. It should be noted that the lattice in $Cu_5(VO_4)_2(OH)_4$ has never been realized in compounds. Therefore, intriguing properties are highly expected in $Cu_5(VO_4)_2(OH)_4$.

Magnetic Properties

Figure 4 shows the temperature dependence of the magnetic susceptibility and the corresponding reciprocal one. The susceptibility increases gradually with decreasing temperature, while a rapid upturn is seen at ~5 K, indicating the inset of a ferromagnetic correlation. A plot of $d\chi/dT$ shows a sharp peak at about 5 K, indicative of a magnetic transition at this temperature (Figure S5). A typical Curie-Weiss behavior is observed above 150 K, giving the Curie constant C =3.18(9) $emu\cdot mol^{-1}\cdot K$ and Weiss constant θ = -152.5(9) K. The negative Weiss constant suggests a dominative antiferromagnetic interaction between neighboring Cu^{2+} ions. The effective magnetic moment of Cu^{2+} ions in the system is calculated to be 2.25(5) μ_B, which is larger than the theoretical spin value of 1.732 μ_B for one isolated Cu^{2+} (S = 1/2) ion with g = 2. This

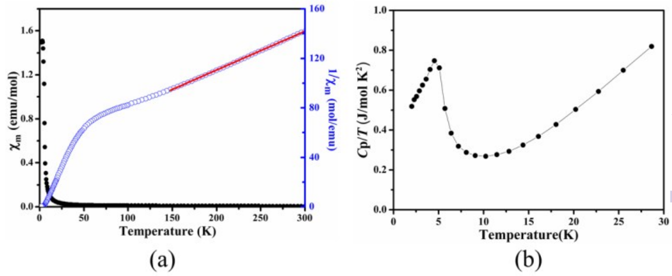

Figure 4. Temperature dependence of the magnetic susceptibility and the corresponding reciprocal for $Cu_5(VO_4)_2(OH)_4$ (a); the heat capacity measured in zero magnetic fields (b).

indicates a large orbital moment contribution of Cu^{2+} in an oxygen octahedral environment. A similar result can also be observed in some CuO-based oxides such as $Cu_5V_2O_{10}$[35] and $BaAg_2Cu[VO_4]_2$,[36] which are suggested to originate from the anisotropic exchanges between Cu^{2+} ions in such distorted CuO_6 octahedra. Heat capacity data (Figure 4b) show a clear sign of λ-like peak around 4.5 K, giving concrete evidence for a long-range AF ordering.

As shown in Figure 5, the value of $\chi_M T$ is observed to be 2.11 $emu\cdot mol^{-1}\cdot K$ at 300 K and decreases gradually with decreasing temperature due to dominant antiferromagnetic interactions. Then a rapid increase is observed at ~5 K and reaches at its maximum with 5.91 $emu\cdot mol^{-1}\cdot K$, confirming the appearance of ferromagnetic component in the system. Such ferromagnetic correlation can also be identified by zero-field-cooled (ZFC) and field-cooled (FC) measurements, which show a bifurcation below the temperatures of ca. 4.5 K (Figure 5 inset). No frequency-dependence was observed in AC measurement, which excludes the spin freezing behavior characteristic of a spin-glass system (Figure S6).

Figure 6 shows the isothermal magnetization as a function of applied field at 2 K. The magnetization shows a rapid increase below about 0.1 kOe and followed by a much slower increase, leading to a magnetization of 0.20 μ_B at 80 kOe, which is 1/5 of saturation value of M_S = 1 μ_B for one Cu(II) ion with S = 1/2. Combing the results of magnetic susceptibility, we can conclude that $Cu_5(VO_4)_2(OH)_4$ exhibits a long-rang ferrimagnetic ordering with 1/5 plateau. Other examples, such as $Co_8(OH)_{12}(SO_4)_2(diamine)\cdot nH_2O$,

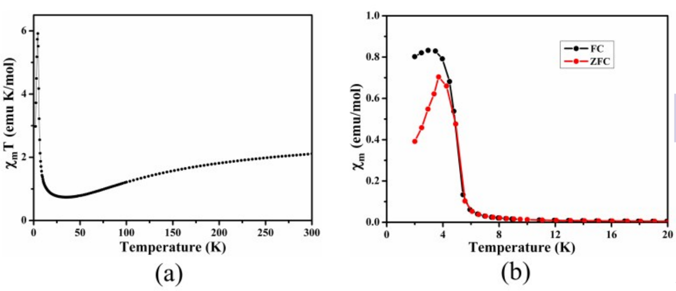

Figure 5. Variation of $\chi_M T$ with the temperature for $Cu_5(VO_4)_2(OH)_4$ (a) and the susceptibility measured with the FC and ZFC regimes (b).

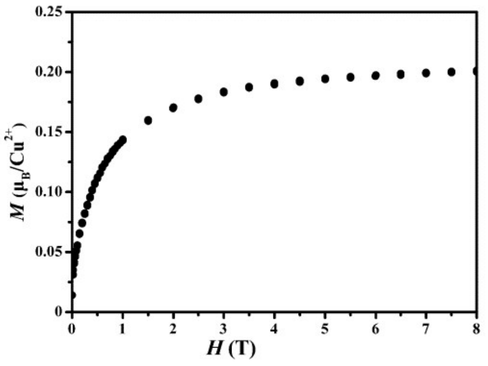

Figure 6. Field magnetization of $Cu_5(VO_4)_2(OH)_4$ up to 8 T measured at 2.0 K.

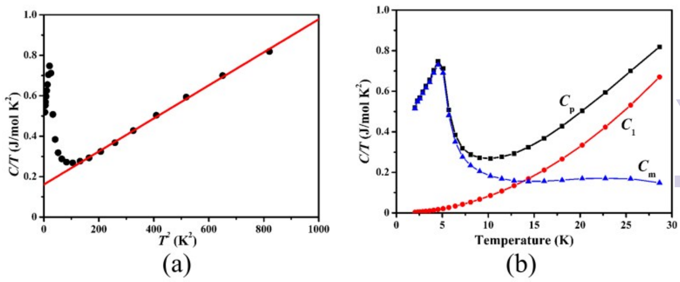

Figure. 8. Linear relation of C/T vs. T^2 above 13 K (a); heat capacity measured in zero magnetic fields. The red line with solid circles represents the lattice contribution (C_l) to heat capacity and blue line with solid triangles is magnetic contribution (C_m) (b).

$Co_5(OH)_8$(1,4-cyclohexanedicarboxylate)$\cdot 4H_2O$, K[$Co_{14}O(OH)_{21}(ox)_3$], $Co_7(OH)_{12}(C_2H_4(SO_3)_2)(H_2O)_2$, and $KCo_{28}(OH)_{43}(ox)_6Br_2(H_2O)_2$ with periodic vacancies in the triangular layer but capped top and bottom by tetrahedral CoO_4 contain ferrimagnetic layers.[37-42] In addition, $Co_5(OH)_6(SeO_4)_2(H_2O)_4$, with a purely 2D triangular network of spins, exhibits ferromagnetic coupling in the layer.[43]

It is noticed that $Cu_5(VO_4)_2(OH)_4$ displays ferrimagnetism with an unusual 1/5 plateau which appears to date only in $CuFeO_2$[44] on triangular lattice with spin-driven bond order and $Cu_5(PO_4)_2(OH)_4$ with a new geometrically frustrated spin-lattice of pentagons and triangles.[45] It is well-known that a typical ferrimagnet usually consists of two heterospin carriers with an antiferromagnetic exchange coupling between the nearest neighbouring magnetic ions. For a homospin system, spin carriers are arranged in special geometrical topologies so that antiferromagnetic interaction cannot cancel the magnetic moments. Thus we suggest the ferrimagnetic ground state with 1/5 magnetization plateau of $Cu_5(VO_4)_2(OH)_4$ may arise from the spin arrangements with up-up-down type for each triangle in the unique spin lattice in it.[46] Therefore, we can presume that the triangular-strips exhibit up-up-down spin arrangements while the honeycomb strips adopt up-down style as shown in Figure 7. The spin alignments give rise to a net magnetic moment of 1/5 (Cu1/Cu2/Cu3=1/2/2) which agrees well with the experimental result.

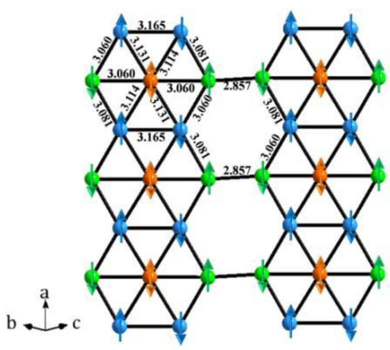

Figure 7. Spin alignments of Cu1 (orange), Cu2 (green) and Cu3 (blue) in spin-lattice of $Cu_5(VO_4)_2(OH)_4$. The distances between Cu^{2+} ions in the triangular and hexagon are labelled.

The special spin arrangements arise from strong spin frustration in the system. We have estimated the frustration by fitting the specific heat and calculating the entropy change. First, we figure out the magnetic contribution, $C_m(T)$, to the specific heat by subtracting the lattice contribution with the Debye model from the raw data C(T). The heat capacity data above 12 K could be fitted to $C_p = \gamma T + \beta_1 T^3$, giving $\gamma = 0.16(1)$ J$\cdot$mol$^{-1}\cdot$K^{-1} and $\beta_1 = 8.17(9) \times 10^{-4}$ J$\cdot$mol$^{-1}\cdot$K^{-4} (Figure. 8a). Since $Cu_5(VO_4)_2(OH)_4$ is an insulator, it is reasonable to arrange the γT term to the magnetic contribution (C_m) and the $\beta_1 T^3$ term to the lattice contribution (C_l). Therefore, the magnetic contribution was calculated as $C_m = C_p - C_l$, and the entropy change associated with the magnetic order was roughly estimated to be ΔS = ~6.8 J$\cdot$mol$^{-1}\cdot$K^{-1}, corresponding to ~23.6% of Rln(2S+1) expected for conventional long-range magnetic ordering spin-1/2 systems, where R is the molar gas constant (Figure. 8b). This result suggests that large amounts of spin fluctuations may still remain below Tc. Generally, for a spin lattice involving triangular, a transition to long-range magnetic order is not theoretically possible at finite temperature due to spin frustration arising from orbital degeneracy. However, the presence of anisotropy, a dipolar field, and/or asymmetric exchange can perturb such a system and introduce some 3D character, which finally results in 3D long-range ordering at finite temperatures.[47,48] In $Cu_5(VO_4)_2(OH)_4$, the character of 2D layer is destroyed and thereby exhibiting 3D long-range ordering. On the one hand, it adopts a low symmetry of *P*-1, resulting in irregular triangles and the nondegeneracy of orbital. Second, the neighboring spin-carrier Cu(II) ions, through the bridging oxygen anions in the unit cell, are not related by an inversion center, resulting the Dzyaloshinsky-Moriya (D-M) interaction, which eliminated the frustration greatly. Finally, the magnetic anisotropy, as demonstrated by the observed effective magnetic moment, is also contributed to the 3D long-rang ordering.

Conclusions

An unprecedented 2D spin lattice of copper(Ⅱ) ions has been discovered in $Cu_5(VO_4)_2(OH)_4$. Most excitingly, it represents a new type of geometrically-frustrated spin lattice featured by alternant triangular strips and honeycomb strips.

To be exactly, it is 1/6 depleted triangular lattice. Its magnetic property has been well studied by magnetic susceptibility, specific heat, field magnetization measurements on the basis of polycrystalline sample. Ferrimagnetic ordering is observed at around 4.5 K. Remarkably, $Cu_5(VO_4)_2(OH)_4$ is a rare example of 1/5 magnetization plateau arising from the unusual competition between antiferromagnetic and ferromagnetic interactions caused by strong frustration. The present work gives new inspirations for exploration of new geometrically-frustrated magnetic systems based on triangular lattice.

Acknowledgements

This work was financially supported by the National Basic Research Program of China (No. 2012CB921701) and National Natural Science Foundation of China (No. 21403234).

References

1 P. W. Anderson, *Science*, 1987, **235**, 1196.
2 K. Kodama, M. Tagigawa, M. Horvatic, C. Berthier, H. Kageyama, Y. Ueda, S. Miyahara, F. Becca, F. Mila, *Science*, 2002, **298**, 395.
3 S. E. Sebastian, N. Harriaon, C. D. Batista, L. Balicas, M. Jaime, P. A. Sharma, N. Kawashima, I. R. Fisher, *Nature*, 2006, **441**, 617.
4 D. G. Nocera, B. M. Bartlett, D. Grohol, D. Papoutsakis, M. P. Shores, *Chem. Eur. J.*, 2004, **10**, 3850.
5 J. E. Greedan, *J. Mater. Chem.*, 2001, **11**, 37.
6 R. Ishii, D. Gautreaux, K. Onuma, Y. Machida, Y. Maeno, S. Nakatsuji, J. Y. Chan, *J. Am. Chem. Soc.*, 2010, **132**, 7055.
7 B. M. Bartlett, D. G. Nocera, *J. Am. Chem. Soc.*, 2005, **127**, 8985.
8 D. Papoutsakis, D. Grohol, D. G. Nocera, *J. Am. Chem. Soc.*, 2002, **124**, 2647.
9 D. Grohol, D. Papoutsakis, D. G. Nocera, *Angew. Chem. Int. Ed.*, 2001, **40**, 1519.
10 W. Miiller, M. Christensen, A. Khan, N. Sharma, R. B. Macquart, M. Avdeev, G. J. McIntyre, R. O. Piltz, C. D. Ling, *Chem. Mater.*, 2011, **23**, 1315.
11 S. Nakatsuji, Y. Nambu, H. Tonomura, O. Sakai, S. Jonas, C. Broholm, H. Tsunetsugu, Y. Qiu, Y. Maeno, *Science*, 2005, **309**, 1697.
12 L. Balents, *Nature*, 2010, **464**, 199.
13 D. E. Freedman, T. H. Han, A. Prodi, P. Müller, Q.-Z. Huang, Y.-S. Chen, S. M. Webb, Y. S. Lee, T. M. McQueen, D. G. Nocera, *J. Am. Chem. Soc.*, 2010, **132**, 16185.
14 S. Chu, T. M. McQueen, R. Chisnell, D. E. Freedman, P. Müller, Y. S. Lee, D. G. Nocera, *J. Am. Chem. Soc.*, 2010, **132**, 5570.
15 M. P. Shores, E. A. Nytko, B. M. Bartlett, D. G. Nocera, *J. Am. Chem. Soc.*, 2005, **127**, 13462.
16 R. H. Colman, A. Sinclair, A. S. Wills, *Chem. Mater.*, 2011, **23**, 1811.
17 D. E. Freedman, R. Chisnell, T. M. McQueen, Y. S. Lee, C. Payen, D. G. Nocer, *Chem. Commun.*, 2012, **48**, 64.
18 H. Yoshida, J.-I. Yamaura, M. Isobe, Y. Okamoto, G. J. Nilsen, Z. Hiroi, *Nat. Commun.*, 2012, **1875**, 1.
19 D. Boldrin, A. S. Wills, *J. Mater. Chem. C*, 2015, **3**, 4308.
20 G. Lawes, A. B. Harris, T. Kimura, N. Rogado, R. J. Cava, A. Aharony, O. Entin-Wohlman, T. Yildirim, M. Kenzelmann, C. Broholm, A. P. Ramirez, *Phys. Rev. Lett.*, 2005, **95**, 087205.
21 J. F. Wang, M. Tokunaga, Z. Z. He, J. I. Yamaura, A. Matsuo, K. Kindo, *Phys. Rev. B*, 2011, **84**, 220407.
22 Y. Okamoto, M. Tokunaga, H. Yoshida, A. Matsuo, K. K. Kindo, Z. J. Hiroi, *Phys. Rev. B*, 2011, **83**, 180407.
23 M. S. Williams, J. P. West, S.-J. Hwu, *Chem. Mater.*, 2014, **26**, 1502.
24 S. Katsura, T. Ide, T. Morita, *J. Stat. Phys.*, 1986, **42**, 381.
25 O. Smirnova, M. Azuma, N. Kumada, Y. Kusano, M. Matsuda, Y. Shimakawa, T. Takei, Y. Yonesaki, N. Kinomura, *J. Am. Chem. Soc.*, 2009, **131**, 8313.
26 E. Climent-Pascual, P. Norby, N. H. Andersen, P. W. Stephens, H. W. Zandbergen, J. Larsen, R. J. Cava, *Inorg Chem.*, 2012, **51**, 557.
27 Y. Miura, R. Hirai, T. Fujita, Y. Kobayashi, M. Sato, *J. Magn. Magn. Mater.*, 2007, **310**, 389.
28 J. X. Xu, A. Assoud, N. Soheilnia, S. Derakhshan, H. L. Cuthbert, J. E. Greedan, M. H. Whangbo, H. Kleinke, *Inorg. Chem.*, 2005, **44**, 5042.
29 E. Sokolova, F. C. Hawthorne, *Can. Mineral.*, 2004, **42**, 731.
30 S. Y. Zhang, W. An, G. Wu, *Chem. Phys. Lett., 2015,* **621***,* 1.
31 A. C. Larson, R. B. Von Dreele, *Los Alamos National Laboratory Report LAUR*, 1994, **86**.
32 B. H. Toby, *J. Appl. Crystallogr.*, 2001, **34**, 210.
33 H. Kabbour, R. David, A. Pautrat, H.-J. Koo, M.-H. Whangbo, G. André, O. Mentré, *Angew. Chem. Int. Ed.*, 2012, **51**, 11745.
34 Z. Z. He, C. S. Lin, W. D. Cheng, A. Okazawa, N. Kojima, J. Yamaura, Y. Ueda, *J. Am. Chem. Soc.*, 2011, **133**, 1298.
35 N. E. Amuneke, D. E. Gheorghe, B. Lorenz, A. Möller *Inorg. Chem.*, 2011, **50**, 2207.
36 A. Aliev, M. Huvé, S. Colis, M. Colmont, A. Dinia, O. Mentré, *Angew. Chem. Int. Ed.*, 2012, **51**, 9393.
37 M. Kurmoo, H. Kumagai, S. M. Hughes, C. J. Kepert, *Inorg. Chem.,* 2003, **42**, 6709.
38 A. Rujiwatra, C. J. Kepert, J. B. Claridge, M. J. Rosseinsky, H. Kumagai, M. Kurmoo, *J. Am. Chem. Soc.*, 2001, **123**, 10584.
39 A. Rujiwatra, C. J. Kepert, M. J. Rosseinsky, *Chem. Commun.*, 1999, 2307. 39.
40 P. M. Forster, M. M. Tafoya, A. K. Cheetham, *J. Phys. Chem. Solids,* 2004, **65**, 11.
41 X.-M. Zhang, X.-H. Zhang, H.-S. Wu, M.-L. Tong and S.W. Ng, *Inorg. Chem.*, 2008, **47**, 7462.
42 T. D. Keene, M. E. Light, M. B. Hursthouseb and D. J. Price, *Dalton Trans.,* 2011, **40**, 2983.
43 M. B. Salah, S. Vilminot, G. André , M. Richard-Plouet, T. Mhiri, S. Takagi, and M. Kurmoo, *J. Am. Chem. Soc.*, 2006, **128**, 7972.
44 T. Nakajima, N. Terada, S. Mitsuda, R. Bewley, *Phys. Rev. B*, 2013, **88**, 134414.
45 H. Kikuchi, N. Thi Tinh Y, A. Matsuo, K. Kindo, *J. Korean Phys. Soc.*, 2013, **62**, 2037.
46 F. Hida, *J. Phys. Soc. Jpn.*, 1994, **63**, 2359.
47 A. Tarantul, B. Tsukerblat, A. Müller, *Inorg. Chem.*, 2007, **46**, 161.

48 J. Yoon, L. M. Mirica, T. D. P. Stack, E. I. Solomon, *J. Am. Chem. Soc.*, 2004, **126**, 12586.

A Frustrated Ferrimagnet $Cu_5(VO_4)_2(OH)_4$ with 1/5 Magnetization Plateau on a New Spin-Lattice of Alternant Triangular Strip and Honeycomb Strip

Su-Yun Zhang, Wen-Bin Guo, Ming Yang, Ying-Ying Tang, Mei-Yan Cui, Nan-Nan Wang, Zhang-Zhen He*

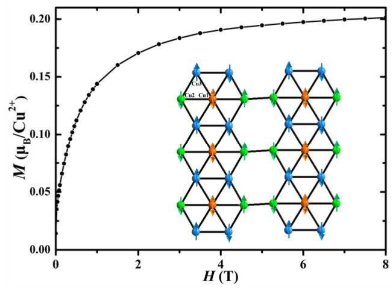

$Cu_5(VO_4)_2(OH)_4$ displays ferrimagnetic with unusual 1/5 magnetization plateau arising from the spin-arrangements of the 1/6 depleted triangular-lattice in it.